

# UCLA

## UCLA Previously Published Works

### Title

Resistance to Ceftazidime-Avibactam Is Due to Transposition of KPC in a Porin-Deficient Strain of *Klebsiella pneumoniae* with Increased Efflux Activity

### Permalink

<https://escholarship.org/uc/item/5vm0t014>

### Journal

Antimicrobial Agents and Chemotherapy, 61(10)

### ISSN

0066-4804

### Authors

Nelson, Kirk  
Hemarajata, Peera  
Sun, Dongxu  
[et al.](#)

### Publication Date

2017-10-01


### DOI

10.1128/aac.00989-17

Peer reviewed



# Resistance to Ceftazidime-Avibactam Is Due to Transposition of KPC in a Porin-Deficient Strain of *Klebsiella pneumoniae* with Increased Efflux Activity

Kirk Nelson,<sup>a</sup>  Peera Hemarajata,<sup>b</sup> Dongxu Sun,<sup>a</sup> Debora Rubio-Aparicio,<sup>a</sup> Ruslan Tsvikovski,<sup>a</sup> Shangxin Yang,<sup>c</sup> Robert Sebra,<sup>d</sup> Andrew Kasarskis,<sup>d</sup> Hoan Nguyen,<sup>e</sup> Blake M. Hanson,<sup>e</sup> Shana Leopold,<sup>e</sup> George Weinstock,<sup>e</sup> Olga Lomovskaya,<sup>a</sup> Romney M. Humphries<sup>b</sup>

The Medicines Company, San Diego, California, USA<sup>a</sup>; Pathology and Laboratory Medicine, University of California, Los Angeles, Los Angeles, California, USA<sup>b</sup>; Department of Pathology, University of New Mexico, Albuquerque, New Mexico, USA<sup>c</sup>; Icahn School of Medicine at Mount Sinai, New York, New York, USA<sup>d</sup>; JAX Genomic Medicine, Farmington, Connecticut, USA<sup>e</sup>

**ABSTRACT** Ceftazidime-avibactam is an antibiotic with activity against serine beta-lactamases, including *Klebsiella pneumoniae* carbapenemase (KPC). Recently, reports have emerged of KPC-producing isolates resistant to this antibiotic, including a report of a wild-type KPC-3 producing sequence type 258 *Klebsiella pneumoniae* that was resistant to ceftazidime-avibactam. We describe a detailed analysis of this isolate, in the context of two other closely related KPC-3 producing isolates, recovered from the same patient. Both isolates encoded a nonfunctional OmpK35, whereas we demonstrate that a novel T333N mutation in OmpK36, present in the ceftazidime-avibactam resistant isolate, reduced the activity of this porin and impacted ceftazidime-avibactam susceptibility. In addition, we demonstrate that the increased expression of *bla*<sub>KPC-3</sub> and *bla*<sub>SHV-12</sub> observed in the ceftazidime-avibactam-resistant isolate was due to transposition of the Tn4401 transposon harboring *bla*<sub>KPC-3</sub> into a second plasmid, pIncX3, which also harbored *bla*<sub>SHV-12</sub>, ultimately resulting in a higher copy number of *bla*<sub>KPC-3</sub> in the resistant isolate. pIncX3 plasmid from the ceftazidime-avibactam resistant isolate, conjugated into a OmpK35/36-deficient *K. pneumoniae* background that harbored a mutation to the *ramR* regulator of the *acrAB* efflux operon recreated the ceftazidime-avibactam-resistant MIC of 32 µg/ml, confirming that this constellation of mutations is responsible for the resistance phenotype.

**KEYWORDS** ceftazidime-avibactam, KPC, *Klebsiella pneumoniae*, porin mutation, resistance

Carbapenemase-producing *Enterobacteriaceae* (CPE) are commonly resistant to all, or nearly all, antibiotics, making treatment of patients with serious infections due to CPE exceedingly difficult. In 2014, the U.S. Food and Drug Administration (FDA) approved ceftazidime-avibactam (Avycaz) for the treatment of complicated urinary tract infections and (when combined with metronidazole) complicated intra-abdominal infections. Avibactam is a novel non-beta-lactam beta-lactamase inhibitor that inactivates class A serine carbapenemase, including the *Klebsiella pneumoniae* carbapenemase (KPC) that is endemic in the United States (1). Avibactam has no activity against class B beta-lactamases. We recently reported the first clinical case of a KPC-3 producing, sequence type 258 *K. pneumoniae* that was resistant to ceftazidime-avibactam (2), recovered from a patient with no history of ceftazidime-avibactam therapy. We established the ceftazidime-avibactam-resistant isolate had higher expression of *bla*<sub>KPC-3</sub> gene compared to a clonal, ceftazidime-avibactam susceptible isolate recovered from

Received 12 May 2017 Returned for modification 30 May 2017 Accepted 6 July 2017

Accepted manuscript posted online 24 July 2017

**Citation** Nelson K, Hemarajata P, Sun D, Rubio-Aparicio D, Tsvikovski R, Yang S, Sebra R, Kasarskis A, Nguyen H, Hanson BM, Leopold S, Weinstock G, Lomovskaya O, Humphries RM. 2017. Resistance to ceftazidime-avibactam is due to transposition of KPC in a porin-deficient strain of *Klebsiella pneumoniae* with increased efflux activity. *Antimicrob Agents Chemother* 61:e00989-17. <https://doi.org/10.1128/AAC.00989-17>.

**Copyright** © 2017 American Society for Microbiology. All Rights Reserved.

Address correspondence to Romney M. Humphries, [rhumphries@mednet.ucla.edu](mailto:rhumphries@mednet.ucla.edu).

**TABLE 1** MICs for KP1245 and KP1244

Antibacterial agent	MIC ( $\mu\text{g/ml}$ ) <sup>a</sup>	
	CRKP #1 (KP1245)	CRKP #2 (KP1244)
Ceftazidime	256 (R)	>1,024 (R)
Ceftazidime-avibactam	4 (S)	32 (R)
Cefepime	32 (R)	512 (R)
Ceftolozane-tazobactam	>256 (R)	>256 (R)
Ceftriaxone	>32 (R)	>32 (R)
Meropenem	16 (R)	512 (R)
Imipenem	8 (R)	>8 (R)
Ertapenem	64 (R)	>64 (R)
Doripenem	16 (R)	>64 (R)
Ampicillin	>32 (R)	>32 (R)
Ampicillin-sulbactam	>32 (R)	>32 (R)
Piperacillin-tazobactam	>256 (R)	>256 (R)
Aztreonam	512 (R)	>1,024 (R)
Amikacin	16 (S)	16 (S)
Gentamicin	1 (S)	2 (S)
Tobramycin	16 (R)	16 (R)
Doxycycline	2 (S)	16 (R)
Minocycline	2 (S)	32 (R)
Tigecycline	1 (S)	8 (R)
Chloramphenicol	$\leq 4$ (S)	>16 (R)
Ciprofloxacin	>2 (R)	>2 (R)
Levofloxacin	16 (R)	64 (R)
Trimethoprim/sulfamethoxazole	$\leq 1/20$ (S)	2/40 (S)
Colistin	0.5 (S)	0.5 (S)

<sup>a</sup>CLSI M100S 27th edition interpretive criteria were used in all cases, with the exception of ceftazidime-avibactam and tigecycline or colistin, where FDA or EUCAST breakpoints were used. R, resistant; S, susceptible.

the same patient. In addition, we found that both isolates carried nonfunctional porin OmpK35 and the ceftazidime-avibactam-resistant isolate harbored a previously undescribed amino acid substitution in the porin OmpK36 (3). In the present study, we demonstrate the increased expression of KPC-3 was a consequence of increased *bla*<sub>KPC-3</sub> gene copy number in the resistant isolate, apparently due to transposition of the *bla*<sub>KPC-3</sub> Tn4401 transposon into a second plasmid, pIncX3, which also harbored *bla*<sub>SHV-12</sub>. We also provide evidence that the novel amino acid substitution in OmpK36 affected this porin's function and that the resistant isolate had enhanced efflux activity. We combined these findings to reconstruct the ceftazidime-avibactam-resistant phenotype, in *K. pneumoniae* strains with porin mutations and enhanced efflux.

## RESULTS AND DISCUSSION

**Bacterial isolates.** Two previously described isolates recovered from the blood of a single patient were analyzed in the present study. These include a ceftazidime-avibactam-susceptible isolate (KP1245, recovered on hospital day 1) and a ceftazidime-avibactam-resistant isolate (KP1244, recovered on day 2) (2). In addition to ceftazidime-avibactam resistance, KP1244 demonstrated higher MICs to non-beta-lactam antibiotics that are known substrates of multidrug efflux pumps (i.e., fluoroquinolones, tetracyclines/glycylcyclines and chloramphenicol) than did KP1245. MICs for the isolates are in Table 1.

We previously demonstrated, by whole-genome sequencing (WGS), that the isolates were clonal, with 17 single nucleotide polymorphisms (SNPs; 7 nonsynonymous) across the genomes (3). In addition to the previously described SNPs, the isolates differed by chromosomal insertions and deletions, including loss of an ~10-kb region, including the *ramA-ramR* operon in isolate KP1245, potentially explaining its increased susceptibility to several antibiotics (see below), and the presence of an insertion sequence between *leuABCD* and its transcriptional regulator, *leuO*, in KP1244. Both isolates contained the same complement of antibiotic resistance genes: *aph(3')-Ia* and *acc(6')-Ib*, which confer resistance to kanamycin and tobramycin, and *mphA*, *drfA14*, and *fosA*, which are responsible for macrolide, trimethoprim, and fosfomicin resistance, respec-

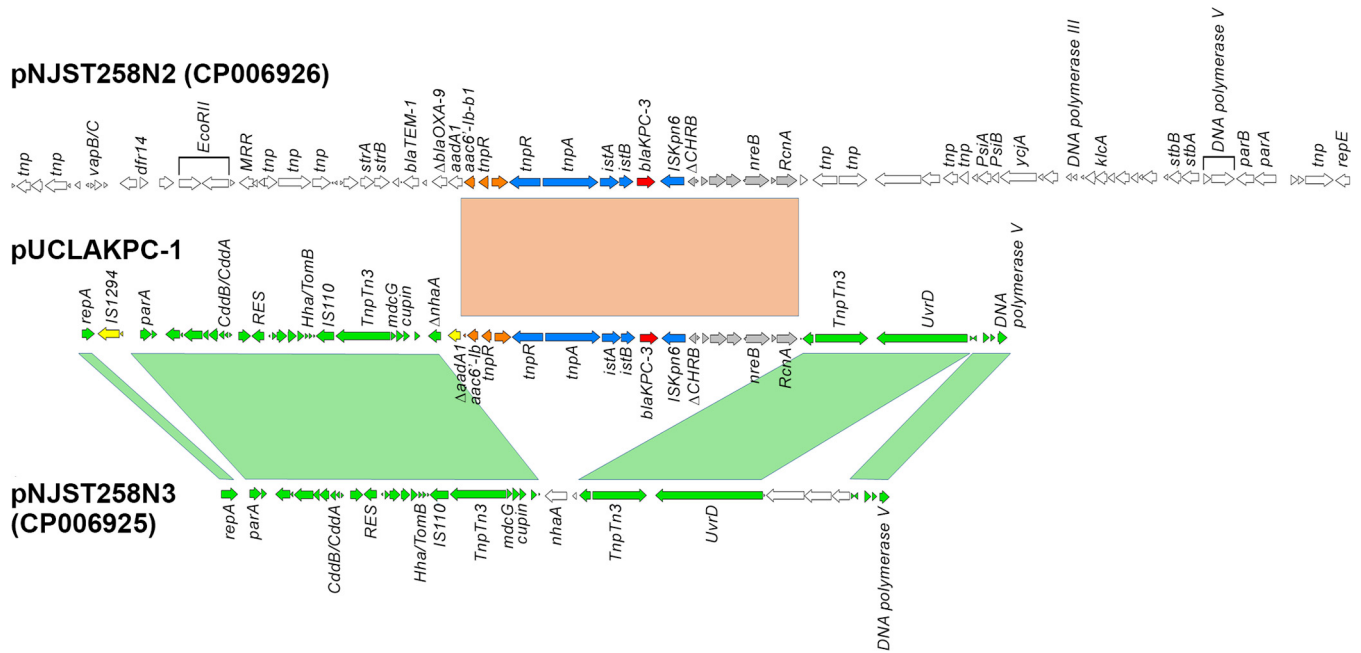


**FIG 1** IncX3 plasmids found in KP1244 and KP1245. pUCLAKPC-2 and pIncX-KP1245 are 66.6- and 55.0-kb plasmids, respectively, with homology to pIncX-SHV (GenBank accession no. [JN247852](#)). pUCLAKPC-2, identified in isolate KP1244, features a Tn4401d insertion in replication initiation protein *repX* at amino acid 7 and a unique IS1294 insertion in the intergenic region between *repX* and *dnaJ*. pUCLAKPC-2 and pIncX-KP1245 share a 9.9-kb region encoding aminoglycoside (*aph3'la*) and macrolide *mph(A)* resistance determinants homologous to two regions of pKPN-a68 ([CP009777](#)) inserted between the genes *umuD* and *bla<sub>SHV-12'</sub>*, as well as an intergenic IS1294 insertion between the gene *dnaJ* and a conserved hypothetical protein, and an SNP, resulting in an early stop for the transcriptional activator gene *actX*. Orange shading marks the region of homology between the Tn4401d from pUCLAKPC-2 and pNJST258N2. Red arrows mark beta-lactamase genes. Dark blue arrows mark the genes of Tn4401. Dark gray arrows and shading mark regions of homology to pKPN-a68. Light blue arrows and shading mark regions of homology to pIncX-SHV. Yellow arrows mark the IS26 and IS1294 transposons.

tively. Both isolates also contained three beta-lactamase genes: *bla<sub>SHV-11'</sub>*, *bla<sub>SHV-12'</sub>*, and *bla<sub>KPC-3'</sub>*. *bla<sub>KPC-3'</sub>* was located within Tn4401, with an identical promoter region of type Tn4401d (3, 4). *bla<sub>SHV-11'</sub>* and *fosA* were present on the chromosomes of both isolates. Of note, a copy of *bla<sub>KPC-3'</sub>::Tn4401d* was identified on the chromosome of KP1245, but not KP1244, disrupting its arylaliphosphatase gene (also called Pter) at nucleotide 707, which was confirmed by PCR (not shown).

**Plasmid content in KP1244 and KP1245.** Plasmid content was analyzed by single molecular long-read sequencing of total DNA by PacBio and MinION platforms to supplement prior estimates obtained by MiSeq data. This analysis yielded a modified interpretation of plasmid content for these two isolates compared to what we previously inferred (3). We now believe three plasmids exist in the two isolates, as opposed to the single IncX3-type plasmid.

First, we confirmed the presence of a pIncX3-type plasmid that carried *bla<sub>SHV-12'</sub>* and had sequence identity with the recently published pIncX-SHV (GenBank accession no. [JN247852](#)) in both isolates KP1244 and KP1245 (5). However, through analysis of the single-molecule sequencing data, we now identified differences between the IncX3 plasmids located in isolates KP1244 and KP1245 (Fig. 1). The plasmid from KP1244 was found to harbor a *bla<sub>KPC-3'</sub>::Tn4401d* element interrupting the *repX* gene, whereas the plasmid from KP1245 did not harbor *bla<sub>KPC-3'</sub>* or a Tn4401 transposon. We named the 66.6-kb plasmid found in isolate KP1244 pUCLAKPC-2 and confirmed the WGS-inferred structure by PCR (GenBank accession no. [KY930325](#)). The *bla<sub>KPC-3'</sub>::Tn4401d* insertion in pUCLAKPC-2 led to the truncation of the replication initiation protein RepX, at amino acid 7. The *bla<sub>KPC-3'</sub>::Tn4401d* sequence is flanked by 5-bp direct repeats, TTTAG, indicating the insertion was the result of a true transposition event. Tn4401 insertions in IncX3 plasmids have been described previously, but in different locations. For instance, pKpS90 ([JX461340](#)) (6) featured a *bla<sub>KPC-2'</sub>::Tn4401a* interrupting the gene *ygbK*, and P45 ([KT362706](#)) (7) contained two *bla<sub>KPC-3'</sub>::Tn4401a*, one interrupting the

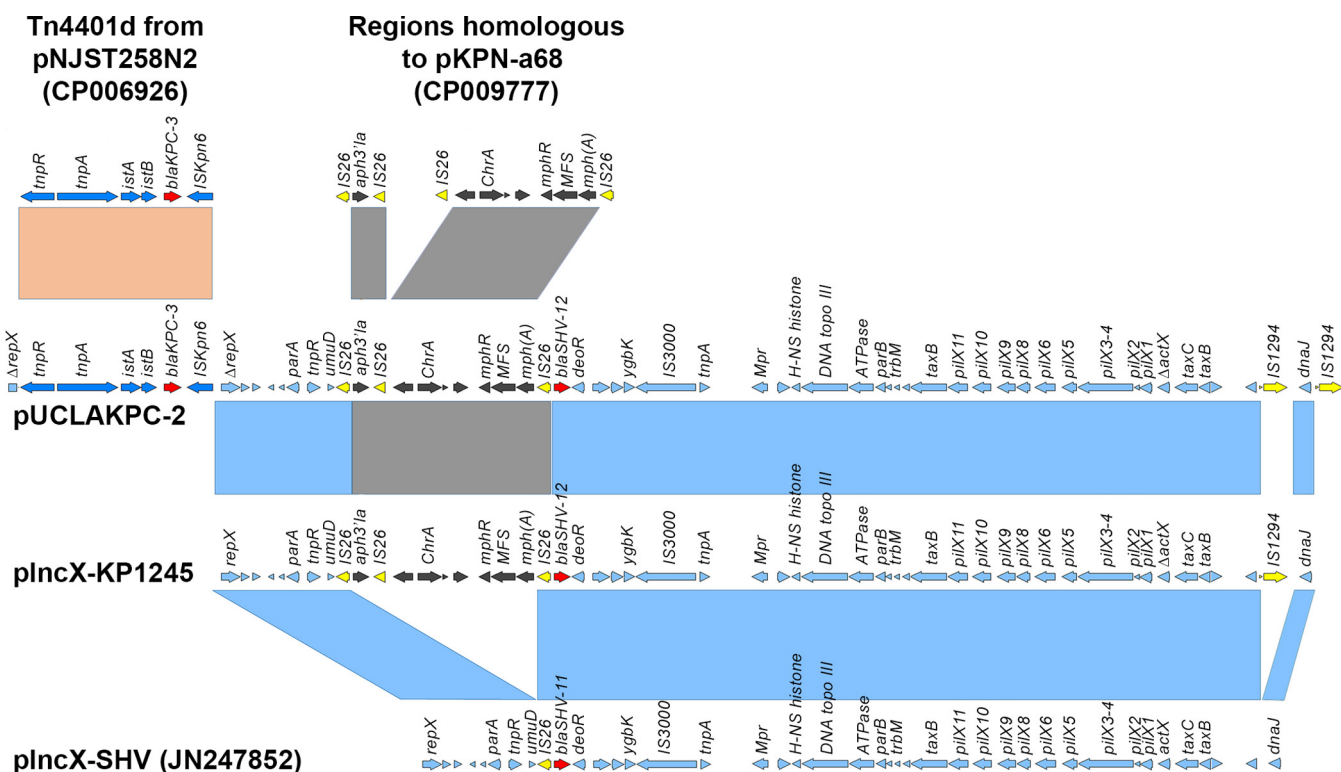


**FIG 2** Plasmid map of pUCLAKPC-1, a 51.2-kb plasmid with large regions of homology to published plasmids pNJST258N2 (GenBank accession no. CP006926) and pNJST258N3 (GenBank accession no. CP006925). Orange shading marks regions of homology between pUCLAKPC-1 and pNJST258N2. Blue arrows mark the genes of Tn4401. Red arrows mark *bla*<sub>KPC-3</sub>. Gray arrows mark nickel, cobalt, and chromium resistance genes. Orange arrows mark genes from the end of Tn4401 to *aac6'*-*lb*. Green arrows and shading mark regions of homology between pUCLAKPC-1 and pNJST258N3. White arrows mark genes in pNJST258N2 and pNJST258N2 without homology in pUCLAKPC-1. Yellow arrows mark genes in pUCLAKPC-1 without homology in pNJST258N2 or pNJST258N3.

gene *IS3000* and another interrupting the gene *topB* (DNA topoisomerase III). Outside the presence of *bla*<sub>KPC-3</sub>::Tn4401d in pUCLAKPC-2 (KP1244), the IncX3 plasmids from isolates KP1244 and KP1245 differed in several regions from plncX-SHV. These included the presence of a 9.9-kb region encoding aminoglycoside (*aph3'**la*) and macrolide (*mphA*) resistance determinants homologous to regions found in pKPN-a68 (CP009777 [8]) (Fig. 1). In addition, the plasmids from both isolates shared an intergenic *IS1294* insertion between the genes encoding *dnaJ* and a conserved hypothetical protein, and an SNP resulting in an early stop for the transcriptional activator gene *actX*. pUCLAKPC-2 harbored a second *IS1294* insertion in an intergenic region between *repX* and *dnaJ* (Fig. 1).

The second plasmid identified in both KP1244 and KP1245 harbored reads of various length homologous to the plasmids pNJST258N2 (carries *bla*<sub>KPC-3</sub>::Tn4401d) and pNJST258N3 (GenBank accession nos. CP006926 and CP006925, respectively) (1). The plasmid from isolate KP1244 we named pUCLAKPC-1. pUCLAKPC-1 is 51,169 bp in length and contains 18.6 kb of sequence homologous to pNJST258N2, including a second copy of Tn4401d::*bla*<sub>KPC-3</sub> in this strain, and also *aac(6')**lb* and genes related to nickel, cobalt, and chromium resistance. Roughly, 31 kb of pUCLAKPC-1 is homologous to pNJST258N3 (Fig. 2). The structure of pUCLAKPC-1 was confirmed by PCR (GenBank accession no. KY930324). KP1245 also contained a plasmid with regions of various lengths with homology to pNJST258N2 and pNJST258N3 (not shown), including Tn4401d::*bla*<sub>KPC-3</sub>. However, KP1245 was found to harbor more regions homologous to pNJST258N2 and fewer regions homologous to the pNJST258N3, relative to KP1244 (Fig. 2).

The differences in *bla*<sub>KPC-3</sub> harboring plasmids between isolates KP1244 and KP1245 was confirmed by transformation experiments. *Escherichia coli* DH5 $\alpha$  transformed with plasmid DNA isolated from isolates KP1244 and KP1245 yielded transformants resistant

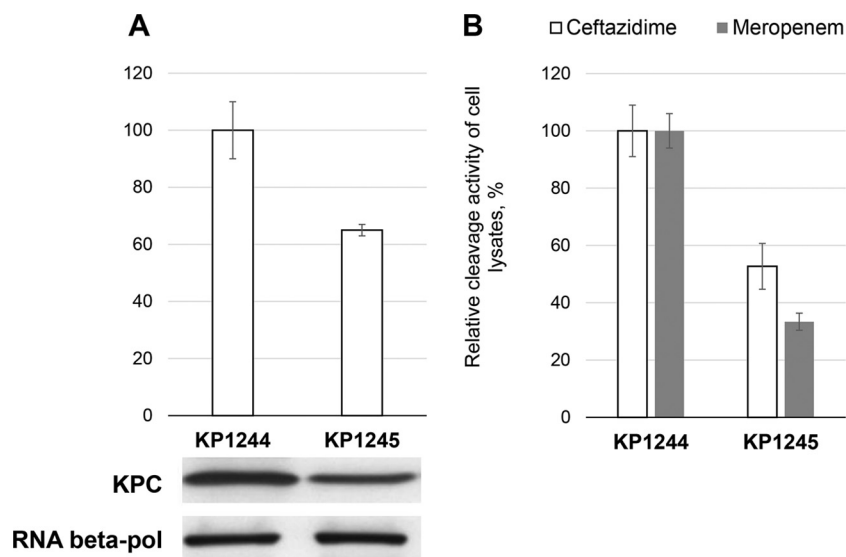


**FIG 3** (A) Relative KPC-3 expression determined by Western blotting, using anti-RNA polymerase B as a loading control, and corresponding expression levels calculated by densitometry analysis from three experiments. (B) Beta-lactamase activities of KP1244 and KP1245. The relative rates of ceftazidime and meropenem hydrolysis by lysates were normalized to that of the lysate prepared from KP1244 (ceftazidime-avibactam-resistant isolate).

to ceftazidime, macrolides (azithromycin and erythromycin), and kanamycin, a result consistent with the acquisition of genes located on *plncX3*, including *bla*<sub>SHV-12</sub>. However, only transformants obtained from KP1244 DNA had increased MICs to carbapenems (data not shown). PCR analysis confirmed the DH5 $\alpha$  transformants obtained from KP1244 plasmid DNA carried *plncX3* with both *bla*<sub>KPC-3</sub> and *bla*<sub>SHV-12</sub> genes, whereas the KP1245 transformants carried the *bla*<sub>SHV-12</sub> gene alone (data not shown). Despite several attempts, transconjugants obtained from all the donor strains carried only *plncX3* plasmids, indicating that pUCLAKPC-1 was not transmissible.

Finally, both isolates contained an identical 88.2-kb plasmid with a high degree (99%) of homology to the recently described plasmid pNJST258C1 (GenBank accession no. CP006922) (1). Unlike pNJST258C1, the plasmid in KP1244 and KP1245 carries *dfrA14*, which was located between the *repA* and the *frmA* glutathione dehydrogenase genes. The structure of this plasmid, named pUCLA3, was confirmed by PCR and has been deposited in GenBank under accession no. KY940546 (not shown).

**KPC-3 expression and beta-lactamase activity are increased in KP1244 versus KP1245.** We previously documented that the expression of *bla*<sub>KPC-3</sub> mRNA in KP1244 was (3.8  $\pm$  0.2)-fold that of isolate KP1245 (3). We sought to evaluate, in the present study, whether this increased mRNA expression correlated with increased KPC-3 protein and ceftazidime and meropenem hydrolysis. KPC-3 protein expression, relative to that of the beta subunit of RNA polymerase, was determined by Western blotting. The KPC-3 level in KP1245 was 64% that of KP1244 ( $P = 0.0012$ , Fig. 3A), confirming elevated KPC-3 expression in KP1244. Similarly, the rates of both ceftazidime (hydrolyzed by both SHV-12 and KPC-3) and meropenem (hydrolyzed by KPC-3) hydrolysis by KP1244 lysates were 1.6- and 2.9-fold higher, respectively, than those of lysates prepared from KP1245 (Fig. 3B).

We next sought to determine the *bla*<sub>KPC-3</sub> gene copy number relative to the genes encoding 16S RNA from log-phase cultures of KP1244 and KP1245. In these experiments, we also included the reference strain KP1074, which contains the *bla*<sub>KPC-3</sub> gene located on a well-characterized low-copy-number plasmid pKpQIL-IL (9). Quantitative real-time PCR (qPCR) experiments performed in triplicate demonstrated that the copy number of *bla*<sub>KPC-3</sub> in KP1244 was 2.7- and 2.4-fold higher, respectively, compared to KP1245 and KP1074 (Fig. 4). This observation contrasts with our previously reported

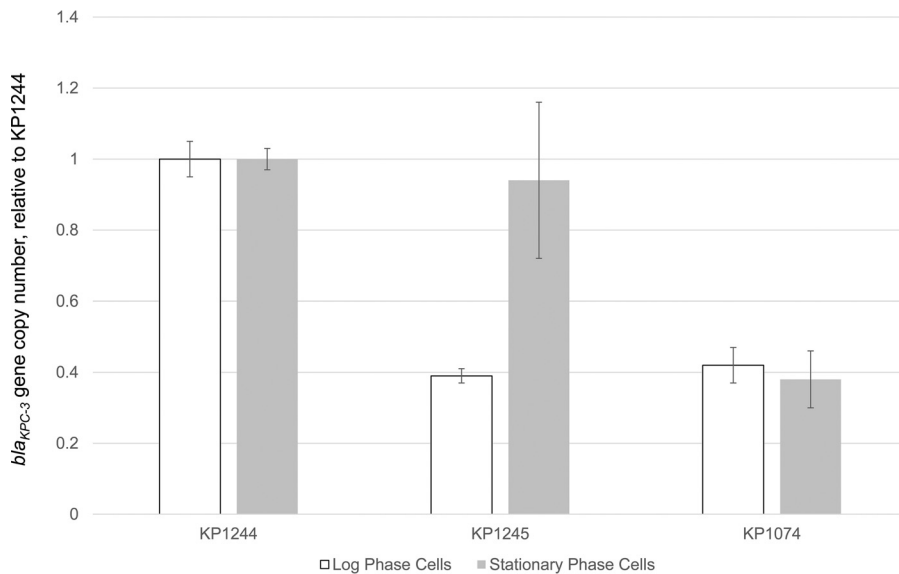


**FIG 4**  $bla_{KPC-3}$  gene copy number in strains KP1245 and KP1074 relative to strain KP1244 in log- and stationary-phase cells.

copy number estimate from WGS read coverage data and reverse transcription-PCR of stationary-phase cells, wherein the copy number was equal (3). We thus determined the copy number of  $bla_{KPC-3}$  in stationary-phase cultures (Fig. 4), which demonstrated no difference in the  $bla_{KPC-3}$  copy number in stationary-phase cultures of the isolates, a finding consistent with the gene copy number estimated based on the depth of read coverage (3). No growth-phase-dependent change in  $bla_{KPC-3}$  was observed for either KP1244 or KP1074. We speculate that this increase in copy number could be related to the site of insertion of Tn4401: the transposon was inserted very close to the 5' end of the gene *repX3* that encodes the replication initiation protein. MIC testing is performed using log-phase cells; hence, the higher copy number and expression of the beta-lactamase genes,  $bla_{KPC-3}$  and  $bla_{SHV-12}$ , observed in log-phase of KP1244 cells appears to be directly related to the increased ceftazidime-avibactam resistance of this isolate compared to other two genetically related strains. qPCR studies to estimate the copy number of the  $bla_{SHV-12}$  gene yielded similar results, corroborating this hypothesis (data not shown). More studies are under way to determine the exact mechanism of the copy number increase of this plasmid.

**Both major porins, OmpK35 and OmpK36, are defective in KP1244 but not in KP1245.** Of the nonsynonymous mutations previously identified in KP1244 versus KP1245 (3), mutations to the outer membrane porins were the most likely contributors to ceftazidime-avibactam resistance. Both isolates harbored mutations predicted to encode R191L in OmpK36 and a nonfunctional OmpK35 due to a frameshift mutation predicted to truncate the protein at amino acid 42. The latter mutation is common to *K. pneumoniae* ST258 (10). However, KP1244 harbored an additional missense mutation near the 3' end of the *ompk36* gene predicted to encode a T333N substitution. A recent report demonstrated an association between the presence of mutations in *ompk36* and elevated ceftazidime-avibactam MICs (11). However, T333N, which is found in one of the beta-sheet domains of the OmpK36 subunit, has not previously been described in *K. pneumoniae*, which prompted us to further investigate the relative impact of this mutation on OmpK36 activity.

Since both KP1244 and KP1245 harbor nonfunctional OmpK35 porins, OmpK36 is the major route of meropenem entry to periplasm. Meropenem hydrolysis by whole cells, compared to lysates, was thus used to evaluate the relative activity of OmpK36. By this analysis, the rate of meropenem uptake by K1245 was 12.5-fold that of KP1244 (Fig. 5). These results are consistent with the deleterious effect of the T333N amino acid

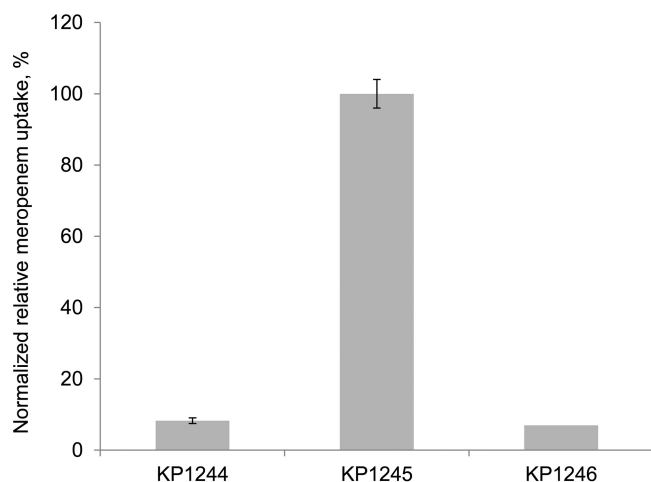


**FIG 5** Uptake of meropenem into the cellular periplasm, normalized to that of KP1245, as an assay for the activity of OmpK36.

substitution on OmpK36 activity. Of note, an inverse correlation between the rate of meropenem uptake and both meropenem and ceftazidime-avibactam MICs was observed (Table 1).

We next evaluated whether T333N contributes to ceftazidime-avibactam resistance in KP1244. Wild-type *ompK36* and *ompK35* genes were transformed into KP1244 and KP1245, and the ceftazidime, ceftazidime-avibactam, and meropenem MICs of the resulting transformants were determined (Table 2). In KP1244, the wild-type *ompK36* reduced the ceftazidime-avibactam and meropenem MICs by 2- and 4-fold, respectively, indicating that the T333N substitution affects susceptibility to these antibiotics, albeit not very significantly. At the same time, no effect of the wild-type *ompK36* was observed when it was introduced into KP1245, indicating that the R191L substitution did not affect OmpK36 activity. The wild-type *ompK35* had a 4- to 16-fold effect on ceftazidime-avibactam and meropenem MIC in both isolates. In KP1245, the wild-type OmpK35 also reduced the ceftazidime MIC by 4-fold. These results demonstrated that complete or partial inactivation of OmpK36 in the background of a nonfunctional OmpK35 may be associated with an increased ceftazidime-avibactam MIC (Table 2).

**Effect of efflux on ceftazidime-avibactam resistance phenotype.** WGS demonstrated that all isolates harbored the AcrAB efflux pump. Interestingly, KP1245 had an ~10-kb deletion of a chromosomal region that included *ramR-ramA* genes; one of the functions of these genes is to regulate expression of the *acrAB* efflux operon (12). The lack of *ramRA* may have accounted for chloramphenicol, doxycycline, and tigecycline susceptibility in this isolate (Table 1). We evaluated the expression of the *acrB* gene, which encodes a component of the AcrAB efflux pump, by RT-qPCR to confirm this finding. The results demonstrated that *acrB* expression in KP1245 was  $(0.19 \pm 0.01)$ -fold that of KP1244 (data not shown).

**TABLE 2** Complementation of *ompK36* and *ompK35* mutations in KP1244 and KP1245

Strain	Description	Meropenem MIC ( $\mu\text{g/ml}$ )	Ceftazidime MIC ( $\mu\text{g/ml}$ ) in the presence of various concns of avibactam ( $\mu\text{g/ml}$ )			
			0	2	4	8
KPM2574	KP1244+vector	256	>128	64	32	8
KPM2573	KP1244+pRX:: <i>ompK36_wt</i>	64	>128	32	16	4
KPM2572	KP1244+pRX:: <i>ompK35_wt</i>	16	>128	8	4	2
KPM2581	KP1245+pUCP24 vector	16	>128	4	2	2
KPM2580	KP1245+pRX:: <i>ompK36_wt</i>	16	>128	4	4	2
KPM2579	KP1245+pRX:: <i>ompK35_wt</i>	4	64	0.5	0.5	0.25



**Reconstruction of the ceftazidime-avibactam resistance phenotype.** To determine whether the combination of an increased KPC-3 activity, a reduced carbapenem uptake, and an increased efflux were sufficient to confer the ceftazidime-avibactam resistance phenotype, we conjugated the pUCLAKPC-2 plasmid from KP1244 into a set of isogenic *K. pneumoniae* strains with defined mutations in porin genes and the AcrAB efflux system. The concentration response of potentiation of ceftazidime by avibactam in the resulting strains was evaluated (Table 3). As a control, we conjugated the same strains with the pKpQIL plasmid from KP1074, which has 2-fold-lower plasmid copy number than pUCLAKPC-2 and does not carry *bla*<sub>SHV-12</sub> (see above).

We first evaluated pUCLAKPC-2 in a wild-type background generating strain KPM2561, with functional porins and a constitutive level of AcrAB expression. The ceftazidime and ceftazidime-avibactam (avibactam fixed at 4  $\mu\text{g/ml}$ ) MICs were 256  $\mu\text{g/ml}$  (resistant) and 1  $\mu\text{g/ml}$  (susceptible), respectively, indicating a 1,024-fold increase in the ceftazidime MIC and an almost complete reversal of ceftazidime resistance by avibactam. In contrast, when the pKpQIL plasmid from KP1074 was transformed into the wild-type background (KPM1271), the ceftazidime MIC was 64  $\mu\text{g/ml}$ , and the ceftazidime-avibactam MIC was 0.5  $\mu\text{g/ml}$  (Table 3).

We next evaluated pUCLAKPC-2 in a series of mutants with increased efflux and porin mutations. In a background of both increased efflux and reduced expression of *ompK35* (KPM2654), the ceftazidime and ceftazidime-avibactam MICs were >256 and 2  $\mu\text{g/ml}$ , respectively. In contrast, the background with pKpQIL was 2-fold more susceptible to ceftazidime-avibactam (Table 3). To determine the relative effect of increased efflux versus decreased expression of OmpK35, we introduced the pUCLAKPC-2 into a background of *ompK35* deletion and normal expression of *acrAB* (strain KPM2656). The ceftazidime and ceftazidime-avibactam MICs in this strain were >256 and 4  $\mu\text{g/ml}$ , respectively, which were slightly higher than for KPM2654, which harbored increased efflux and downregulated OmpK35. These results indicated that the *ompK35* mutation alone was sufficient to increase the ceftazidime-avibactam MIC by at least 4-fold compared to a wild-type background. Deleting *ompK35* from the strain with *ramR* mutation also had an additional 2-fold effect (KPM2656 versus KPM2632, Table 3), likely because the complete inactivation of *ompK35* had a somewhat stronger effect than the *ramR* mutation, leading to the repression of *ompK35* expression. The corresponding pKpQIL-like containing transconjugants KPM2601 and KPM2628 remained 2-fold more susceptible to ceftazidime-avibactam than the respective pUCLAKPC-2 transconjugants.

The effect of OmpK36 inactivation on ceftazidime-avibactam resistance was evaluated by introducing pUCLAKPC-2 into an OmpK36-deficient strain that also harbored the same *ramR* mutation as KPM2654 (strain KPM1171, Table 3). The resulting transconjugant, KPM2566, had a ceftazidime-avibactam MIC of 32  $\mu\text{g/ml}$ , which was the same as that of the ceftazidime-avibactam-resistant patient isolate KP1244 (32  $\mu\text{g/ml}$ ), which was tested in parallel. Compared to KPM2654, KPM2566 had a 16-fold increase in ceftazidime-avibactam MIC, the strongest observed single-step increase, indicating the significant impact of OmpK36, at least in a background of reduced expression of OmpK35 and increased efflux. An MIC of 32  $\mu\text{g/ml}$  was also observed in the pUCLAKPC-2 transconjugated strain KPM2633, which was an OmpK35-deficient derivative of KPM2566 (i.e., an OmpK35- and OmpK36-deficient strain with a *ramR* mutation, called KPM2611). Interestingly, two pKpQIL-containing transconjugants that had the same background as KPM2566 and KPM2633, i.e., KPM1273 and KPM2629, respectively, had 4-fold-lower ceftazidime-avibactam MICs compared to pUCLAKPC-2-containing transconjugants, with a susceptible MIC of 8  $\mu\text{g/ml}$ . This somewhat larger difference between the strains of similar backgrounds that carried pUCLAKPC-2 and the pKpQIL-like plasmid might be due to a stronger effect of the plasmid copy number when other resistance mechanisms, such as porin mutations and increased efflux, occur in the same cell. Alternatively, the effect of increased efflux or the presence of SHV-12 might become more important in the presence of additional mechanisms, such mutation to both OmpK35 and OmpK26, and the presence of KPC. Taken together, the results demonstrate how

**TABLE 3** Ceftazidime-avibactam MICs against *K. pneumoniae* in a variety of backgrounds conjugated with either the IncX-*bla*<sub>KPC-3</sub> plasmid from a ceftazidime-avibactam-resistant clinical isolate (KP1244) or the pKpQIL plasmid from reference strain KP1074<sup>a</sup>

Strain	Origin/construction	Recipient	Donor	OmpK35	OmpK36	<i>acrAB</i>	Ceftazidime MIC (mg/liter) in the presence of various avibactam concns (mg/liter)				
							0	1	2	4	8
KPM2561	This study	KPM1026A	KP1244	F	F	Basal	256	2	2	1	0.5
KPM1271	This study	KPM1026A	KP1074	F	F	Basal	64	1	1	0.5	0.5
KPM2654	This study	KPM1027 (KPM1026 <i>ramR</i> <sup>b</sup> )	KP1244	Down	F	Up	>256	8	4	2	0.25
KPM1272	This study	KPM1027 (KPM1026 <i>ramR</i> )	KP1074	Down	F	Up	256	4	2	1	0.25
KPM2656	This study	KPM2600 (KPM1026a $\Delta$ ompK35)	KP1244	NF	F	Basal	>256	16	8	4	2
KPM2601	This study	KPM2600 (KPM1026a $\Delta$ ompK35)	KP1074	NF	F	Basal	256	8	4	2	1
KPM2632	This study	KPM2610 (KPM1027 $\Delta$ ompK35)	KP1244	NF	F	Up	>256	8	4	2	0.25
KPM2628	This study	KPM2610 (KPM1027 $\Delta$ ompK35)	KP1074	NF	F	Up	256	4	2	1	0.25
KPM2566	This study	KPM1171 (KPM1027 $\Delta$ ompK35)	KP1244	Down	NF	Up	>256	256	64	32	8
KP1273	This study	KPM1171 (KPM1027 $\Delta$ ompK35)	KP1074	Down	NF	Up	>256	32	16	8	4
KPM2633	This study	KPM2611 (KPM1171 $\Delta$ ompK35)	KP1244	NF	NF	Up	>256	256	64	32	8
KPM2629	This study	KPM2611 (KPM1171 $\Delta$ ompK35)	KP1074	NF	NF	Up	>256	32	16	8	4
KP1244	Humphries et al. (2)	NA	NA	NF (ompK35_FS42)	ompK36_1244 (R191L, T333N)	Up	>256	>256	128	32	8
K1074	ATCC BAA-2814	NA	NA	NF (ompK35_FS42 <sup>d</sup> )	ompK36_GD <sup>e</sup>	Basal	>256	16	4	2	1

<sup>a</sup>Abbreviations: NA, not applicable; F, functional; NF, nonfunctional; Down, downregulated; Up, upregulated; Basal, basal level of expression.

<sup>b</sup>An 8-bp insertion in *ramR* caused a frameshift from amino acid 46. This mutation results in overexpression of the *acrAB* efflux operon.

<sup>c</sup>OmpK36.1171 lacks 16 C-terminal amino acids, resulting in a nonfunctional protein; KPM1171 was selected from KPM1027 on meropenem at 0.25  $\mu$ g/ml.

<sup>d</sup>OmpK35\_FS42 has a 1-bp insertion that results in a frameshift from amino acid 42.

<sup>e</sup>OmpK36.1074 has a two-amino-acid insertion, Gly134Asp135, in the L3 loop of the protein, leading to the narrowing of the channel aperture.

a combination of multiple mechanisms, each providing an incremental MIC increase, can result in resistance to ceftazidime-avibactam.

**Summary.** Detailed analysis of the two closely related clinical isolates described in this study demonstrated that, in the background of a nonfunctional OmpK35, inactivation of OmpK36 when combined with increased expression of *bla*<sub>KPC-3</sub> and *bla*<sub>SHV-12</sub> can result in ceftazidime-avibactam resistance. Although surveillance studies continue to document very low rates of resistance to ceftazidime-avibactam among the *Enterobacteriaceae* (13), testing ceftazidime-avibactam is not common in microbiology laboratories, and resistance may be underappreciated. Resistance documented to date has largely been attributed to sporadic occurrence of class B beta-lactamases, against which ceftazidime-avibactam has no activity (14). For instance, a recent report documented the endemic presence of NDM-expressing CPE at a large hospital in Texas, which was identified by testing ceftazidime-avibactam (15). In addition, recent reports by Shields et al. documented several cases of ceftazidime-avibactam treatment failures due to *K. pneumoniae* isolates that had acquired mutation to the omega loop of KPC-3, which resulted in increased ceftazidime hydrolysis and consequent resistance to ceftazidime-avibactam (16, 17).

We demonstrate here that resistance to ceftazidime-avibactam can also occur due to the combination of multiple resistance mechanisms, which could be easily selected by the treatment with various antibiotics. Mutations in *ompK35* are commonly observed in ESBL (extended-spectrum beta-lactamase)- and KPC-producing isolates (18). The emergence of *ompK36* mutations in the strains that lack OmpK35 during treatment with carbapenems is well documented (19, 20). Our patient had no exposure to ceftazidime-avibactam but had undergone extensive prior treatment with meropenem and cefepime (2), which may have provided the selective pressure required for a mutation to OmpK36 and movement of the Tn4401d transposon and increased KPC-3 activity, the collateral damage of this being resistance to ceftazidime-avibactam. Castanheira et al. have also recently reported a KPC-2-expressing isolate whose ceftazidime-avibactam resistance was attributed to decreased expression of *ompK36* and a premature stop codon in *ompK35* (14). Similarly, Shen et al. recently evaluated a large collection of KPC-producing clinical isolates from China that belong to ST-11 and concluded that the decreased ceftazidime-avibactam susceptibility was caused by high ceftazidime hydrolysis activity and OmpK35 porin deficiency (21), a conclusion consistent with our own observations. Although these researchers did not describe any isolates with frank ceftazidime-avibactam resistance, the collection evaluated contained several isolates similar to KP1245. Our study demonstrates how an additional mutation in *ompK36* and/or further increase in KPC copy number can easily result in a clinically resistant phenotype. It remains to be seen whether or not this multifactorial resistance will emerge during treatment. However, since resistant strains appear to preexist in a population, testing for ceftazidime-avibactam susceptibility emerges as an essential step in making treatment decisions.

## MATERIALS AND METHODS

**Bacterial isolates and *in vitro* susceptibility testing.** Bacterial isolates were subjected to broth microdilution susceptibility testing, performed according to Clinical and Laboratory Standards Institute (CLSI) methods (22), using panels prepared in-house. Antimicrobial susceptibility results were interpreted according to CLSI M100S 27th edition breakpoints (22), with the exception of ceftazidime-avibactam and tigecycline, which were interpreted using FDA breakpoints. Colistin MICs were interpreted using the EUCAST *Enterobacteriaceae* breakpoint of <4 µg/ml to indicate susceptibility.

**Whole-genome sequencing and data analysis.** Genomic DNA was prepared using EZ1 Biorobot with a DNA tissue kit (Qiagen, Valencia, CA). DNA sequencing was performed by single-molecule real-time sequencing on PacBio RSII using C4-P6 chemistry and enzyme (Menlo Park, CA) and by an Oxford Nanopore (Oxford Nanopore Technologies, Oxford, UK) system to confirm plasmid structure with orthogonal long-read sequencing approaches. Reads were mapped against the reference chromosome of *K. pneumoniae* 32192 (NCBI accession number CP010361.1). Resistance genes were identified by submitting contigs to ResFinder (23). Assembled contigs were submitted to PlasmidFinder (24) to identify origins of replication that could be found in an *Enterobacteriaceae*-compatible plasmid. Raw reads were processed on the Galaxy server (25) using FASTQ Groomer (26), followed by FASTQ Joiner (26) to match and merge paired reads.

**Determination of transcription levels of *acrB* and *infB*.** Single colonies from an overnight plate were inoculated into CA-MHB and grown at 37°C until an optical density at 600 nm (OD<sub>600</sub>) of 0.7 was

obtained. Cell pellets were collected by centrifugation, and total RNA was isolated by using an Ambion RiboPure-Bacteria RNA isolation kit (Thermo Fisher, San Diego, CA). Residual DNA in the RNA samples was removed by treatment with DNase I according to the manufacturer's instructions. Reverse transcription (RT) was performed using TaqMan reverse transcriptase reagent kit (Thermo Fisher). A mixture of primers for genes to be tested (*acrB* and *infB*) (see Table S1 in the supplemental material), each at a final concentration of 0.5  $\mu\text{M}$ , was used as RT primers. The RT reaction mixture was diluted 10-fold and used in quantitative real-time PCR (qPCR) performed on an ABI Prism 7000 Sequence (Applied Biosystems) using SYBR Select master mix (Thermo Fisher). For these reactions, 9  $\mu\text{l}$  of the diluted RT reaction mixture was used as the template and mixed with 10  $\mu\text{l}$  of SYBR Select master mix ( $2\times$ ) and 1  $\mu\text{l}$  of a qPCR primer pair mix to make the final concentration of forward and reverse primers at 0.5  $\mu\text{M}$  were used. qPCRs were performed in duplicate as described above. The reference gene *infB*, encoding translation initiation factor 2, was used as the internal control for qPCR signal normalization. Relative transcripts levels were calculated by using the  $2^{-\Delta\Delta C_T}$  method (27). At least three independent RNA samples isolated from three separate cultures were used to determine the average transcript levels of each strain.

**Determination of relative *bla*<sub>KPC-3</sub> and *bla*<sub>SHV-12</sub> gene copy numbers.** To compare the *bla*<sub>KPC-3</sub> and *bla*<sub>SHV-12</sub> gene copy numbers between bacterial isolates and between logarithmic phase and stationary-phase cells, a single colony was inoculated into cation-adjusted Mueller-Hinton broth and grown with shaking at 37°C until either the logarithmic (estimated by an OD<sub>600</sub> of 0.5) or the stationary (10 h of incubation) phase of growth was obtained. Cells were harvested from a 0.3-ml aliquot of the culture by a 1-min centrifugation and resuspended in 0.1 ml of water. The suspension was heated at 95°C for 10 min and stored at -20°C for future use as the template in quantitative PCR. qPCR was performed on ABI Prism 7000 sequence (Applied Biosystems) using SYBR Select master mix (Thermo Fisher). The template preparations were diluted 10-fold with water, and 9  $\mu\text{l}$  of the dilution was used in a qPCR which also contained 10  $\mu\text{l}$  of SYBR Select master mix ( $2\times$ ) and 1  $\mu\text{l}$  of a qPCR primer pair mix to make the final concentration of forward and reverse primers at 0.5  $\mu\text{M}$ . The primers Univ-5-qF and Univ-5-qR, representing a conserved region of the bacterial 16S rRNA gene, were used as internal control. The qPCR was run in duplicate with the following thermal cycling conditions: 50°C for 2 min and 95°C for 5 min, followed by 40 cycles of 95°C for 15 s, 55°C for 15 s, and 70°C for 45 s.

The qPCR result ( $C_T$  value) of *bla*<sub>KPC-3</sub> and *bla*<sub>SHV-12</sub> genes of each isolate were subtracted from the  $C_T$  value of the internal control (Univ-5 primers). The difference ( $\Delta C_T$ ) was used as a logarithmic power (base = 2) to calculate the relative signal strength of KPC gene in the isolate. The values were multiplied by 1,000 and used for comparison among different isolates. At least three independent cultures were used to determine average gene signal strength of each strain. All qPCR testing performed conformed with MIQE guidelines (28).

**Cloning of *ompK36* and *ompK35* genes and transformation.** The coding sequences of *ompK35* and *ompK36* genes from *K. pneumoniae* KPM1026a were amplified using the primer pairs KP-ompK35-clone (forward, 5'-CAGGAAGCTTATGATGAAGCGCAATATTCTGG-3'; reverse, 5'-ACGCTCTAGATGTAGA ACTGGTAAACGATACCC-3') and KP-ompK36-clone (forward, 5'-CCGAAGCTTATGAAAGTTAAAGTACT GTCCC-3'; reverse, 5'-CGCATCTAGATTAGAACTGGTAAACCAGGC-3'), respectively, and cloned into the pCR-Blunt vector (Thermo Fisher). After verification of the nucleotide sequence, the recombinant plasmids were digested with restriction enzymes HindIII and XbaI, and the *ompK35* and *ompK36* coding sequences were subcloned into restriction-digested expression vector pRX1 under the IPTG (isopropyl- $\beta$ -D-thiogalactopyranoside)-inducible promoter on the plasmid. The *E. coli* transformants were selected on Luria-Bertani (LB) agar containing gentamicin at 15  $\mu\text{g}/\text{ml}$ . The recombinant plasmids were transformed into *K. pneumoniae* strains, which were made competent by CaCl<sub>2</sub> treatment. The transformants were selected on LB agar plates containing gentamicin at 15 to 50  $\mu\text{g}/\text{ml}$ . The MICs for the recombinant strains were determined in the presence of IPTG at 100  $\mu\text{M}$ .

**Conjugation experiments.** The native plasmids carrying *bla*<sub>KPC-3</sub> from either KP1244 (ceftazidime-avibactam-resistant isolate) or from KP1074 (the reference strain that carries pKpQIL-IL) were introduced into streptomycin-resistant recipient strains with a variety of porin and efflux backgrounds (see Table S4 in the supplemental material) by conjugation to evaluate the impact of porin mutation and efflux on ceftazidime-avibactam resistance. Both donor and recipient strains were grown in LB broth at 37°C with shaking overnight. Then, 50  $\mu\text{l}$ -portions of donor culture were mixed with 50  $\mu\text{l}$  of recipient culture, followed by centrifugation for 1 min at 5,000 rpm at room temperature. After removal of the supernatant, the cells were resuspended in 50  $\mu\text{l}$  of LB medium and spotted onto an LB agar plate without antibiotics. The plate was incubated at 37°C for 4 to 5 h to form a bacterial lawn of growth. The cells were harvested and resuspended in 1 ml of LB medium to achieve an OD<sub>600</sub> of 0.2 to 0.5. Resuspended cells (0.1 ml) were plated on LB agar plates containing 1,000  $\mu\text{g}/\text{ml}$  streptomycin and 8  $\mu\text{g}/\text{ml}$  aztreonam to inhibit both parental strains but allow the growth of transconjugants, which were verified by PCR for the presence of *bla*<sub>KPC</sub>.

**Transformation of native plasmids.** Native plasmids were isolated from bacterial cells using Qiagen Plasmid Midi kit. The plasmid DNA was transformed into *Escherichia coli* DH5 $\alpha$  competent cells prepared by routine CaCl<sub>2</sub> treatment. Transformants were selected on LB agar plates containing ampicillin at 100  $\mu\text{g}/\text{ml}$ . The presence of beta-lactamase genes in the transformants were examined by PCR analysis using the primers listed in Table S1 in the supplemental material.

**Beta-lactamase activity in cell lysates.** Beta-lactamase activity in the clinical isolates was determined by evaluating ceftazidime (for SHV-12 and KPC-3) and meropenem (for KPC only) hydrolysis by cell lysates. Cell suspensions at an OD<sub>600</sub> of 4.0 were sonicated at maximum power twice for 1 min with 5-min rest intervals on ice. Then, 25  $\mu\text{l}$  of lysate was combined with 125  $\mu\text{l}$  of buffer B (50 mM sodium phosphate [pH 7.0], 0.1 mg of bovine serum albumin/ml) in a UV-transparent 96-well plate and

preincubated in a plate reader at 37°C for 10 min. Next, 50  $\mu$ l of a 400- $\mu$ g/ml ceftazidime or meropenem solution in buffer B prewarmed at 37°C (making the final meropenem assay concentration 100  $\mu$ g/ml) was added, and the absorbance at 260 or 294 nm, respectively, was recorded every 15 s for 1 h on a SpectraMax384 plate reader, using eight biological replicates. The initial cleavage rates (OD units/min) were calculated from two OD values located on the linear range of the cleavage curves. To account for spontaneous meropenem degradation, the same meropenem solution was combined with 150  $\mu$ l of buffer C (50 mM sodium phosphate [pH 7.0], 0.5% glucose, 1 mM MgCl<sub>2</sub>) and processed alongside the test samples. *P* values were calculated using *t* test distribution in Excel software.

**KPC-3 Western blots.** Log-phase bacterial cells were diluted to an OD<sub>600</sub> of 0.5, 500 ml of cell culture was spun down, and the resulting pellet was resuspended in 200 ml of 1 $\times$  gel-loading buffer. Then, 20- $\mu$ l portions of cell lysate were loaded on 8 to 16% SDS-PAGE gels, with three replicates for each sample. After gel transfer, the membrane was probed with custom-produced polyclonal rat anti-KPC antibodies (raised using purified recombinant nontagged KPC-2) and subsequently treated with secondary goat anti-rat horseradish peroxidase (HRP)-conjugated antibodies. An anti-RNA polymerase-beta monoclonal antibody HRP conjugate (BioLegend, San Diego, CA) was used as a loading control. Membranes were developed using 1-Step Ultra TMB-Blotting solution (Thermo Fisher). Quantitation of protein expression level was performed by densitometry of Western blot images using 1DscanEX software. Densitometry values from anti-RNA polymerase-beta loading were used for normalization. The relative expression numbers were calculated with the KP1244 level as 100%. Statistical analysis was performed using a *t* test in Excel software.

**Measurement of meropenem uptake in whole cells of *K. pneumoniae*.** Meropenem uptake was measured as a function of hydrolysis by whole cells. Several colonies of each strain from a fresh overnight plate were resuspended in 50 ml of LB medium to get a starting OD<sub>600</sub> of 0.03 to 0.05. Cells were grown at 37°C with shaking at 300 rpm for approximately 3 to 4 h to reach an OD<sub>600</sub> of 0.8 to 0.9. Cells were centrifuged at 5,000 rpm for 10 min at room temperature, and the supernatant was discarded. The resulting cell pellet was washed by centrifugation twice with 25 ml of buffer A (50 mM sodium phosphate [pH 7], 0.5% glucose, 1 mM MgCl<sub>2</sub>), and the final pellet was resuspended in 2.5 ml of buffer A. Then, 100  $\mu$ l of this suspension was diluted in 900  $\mu$ l of buffer B, and the OD<sub>600</sub> was measured. Using the measured OD value, the original suspension was diluted with buffer A to produce an OD<sub>600</sub> of 4, which was used for uptake experiments. Next, 50  $\mu$ l of meropenem at 400  $\mu$ g/ml prepared in buffer A was mixed with 100  $\mu$ l of buffer A in a single well of a clear UV-transparent 96-well plate. A total of 50  $\mu$ l of prepared cell suspension (OD<sub>600</sub> = 4) was added (making the final meropenem assay concentration 100  $\mu$ g/ml), and the absorbance signal at 294 nm was recorded every 30 s for 1 h on a SpectraMax384 plate reader. Absorbance signal decrease profiles (OD<sub>294</sub> versus time) were plotted and used for rate calculation. Initial uptake rates (OD units/min) were calculated from two OD<sub>294</sub> values located on the linear range of the uptake curve. The experiment was performed with eight replicates. Next, meropenem uptake was normalized by intrinsic carbapenemase activity in cell lysates to account for the difference in carbapenemase expression/activity in various strains: meropenem hydrolysis rates obtained in whole-cell experiments were divided by meropenem hydrolysis rates in cell-free lysates. *P* values were calculated with *t* test distribution in Excel software.

**Accession number(s).** The Whole Genome Shotgun projects have been deposited at DDBJ/ENA/GenBank under accession numbers [NELR00000000](https://doi.org/10.1093/nar/nkz000) and [NELS00000000](https://doi.org/10.1093/nar/nkz000) for KP1244 and KP1245, respectively. The sequences of pUCLAKPC-1, pUCLAKPC-2, and pUCLA3 were deposited in GenBank under accession numbers [KY930324](https://doi.org/10.1093/nar/nkz000), [KY930325](https://doi.org/10.1093/nar/nkz000), and [KY940546](https://doi.org/10.1093/nar/nkz000), respectively.

## SUPPLEMENTAL MATERIAL

Supplemental material for this article may be found at <https://doi.org/10.1128/AAC.00989-17>.

**SUPPLEMENTAL FILE 1**, PDF file, 0.3 MB.

## REFERENCES

- Deleo FR, Chen L, Porcella SF, Martens CA, Kobayashi SD, Porter AR, Chavda KD, Jacobs MR, Mathema B, Olsen RJ, Bonomo RA, Musser JM, Kreiswirth BN. 2014. Molecular dissection of the evolution of carbapenem-resistant multilocus sequence type 258 *Klebsiella pneumoniae*. *Proc Natl Acad Sci U S A* 111:4988–4993. <https://doi.org/10.1073/pnas.1321364111>.
- Humphries RM, Yang S, Hemarajata P, Ward KW, Hindler JA, Miller SA, Gregson A. 2015. First report of ceftazidime-avibactam resistance in a KPC-3-expressing *Klebsiella pneumoniae* isolate. *Antimicrob Agents Chemother* 59:6605–6607. <https://doi.org/10.1128/AAC.01165-15>.
- Humphries RM, Hemarajata P. 2017. Resistance to ceftazidime-avibactam in *Klebsiella pneumoniae* due to porin mutations and the increased expression of KPC-3. *Antimicrob Agents Chemother* 61:e00537-17. <https://doi.org/10.1128/AAC.00537-17>.
- Naas T, Cuzon G, Truong HV, Nordmann P. 2012. Role of ISKpn7 and deletions in *bla*<sub>KPC</sub> gene expression. *Antimicrob Agents Chemother* 56:4753–4759. <https://doi.org/10.1128/AAC.00334-12>.
- Garcia-Fernandez A, Villa L, Carta C, Venditti C, Giordano A, Venditti M, Mancini C, Carattoli A. 2012. *Klebsiella pneumoniae* ST258 producing KPC-3 identified in Italy carries novel plasmids and OmpK36/OmpK35 porin variants. *Antimicrob Agents Chemother* 56:2143–2145. <https://doi.org/10.1128/AAC.05308-11>.
- Kassis-Chikhani N, Frangeul L, Drieux L, Sengelin C, Jarlier V, Brisse S, Arlet G, Decré D. 2013. Complete nucleotide sequence of the first KPC-2 and SHV-12-encoding IncX plasmid, pKp590, from *Klebsiella pneumoniae*. *Antimicrob Agents Chemother* 57:618–620. <https://doi.org/10.1128/AAC.01712-12>.
- Fortini D, Villa L, Feudi C, Pires J, Bonura C, Mammaia C, Endimiani A, Carattoli A. 2015. Double copies of Tn4401a:*bla*<sub>KPC-3</sub> on an IncX3 plasmid in *Klebsiella pneumoniae* successful clone ST512 from Italy. *Antimicrob Agents Chemother* 60:646–649. <https://doi.org/10.1128/AAC.01886-15>.
- Conlan S, Thomas PJ, Deming C, Park M, Lau AF, Dekker JP, Smitkin ES, Clark TA, Luong K, Song Y, Tsai YC, Boitano M, Dayal J, Brooks SY, Schmidt B, Young AC, Thomas JW, Bouffard GG, Blakesley RW, Program NCS, Mullikin JC, Korlach J, Henderson DK, Frank KM, Palmore TN, Segre JA.

2014. Single-molecule sequencing to track plasmid diversity of hospital-associated carbapenemase-producing *Enterobacteriaceae*. *Sci Transl Med* 6:254ra126. <https://doi.org/10.1126/scitranslmed.3009845>.
9. Leavitt A, Chmelnitsky I, Carmeli Y, Navon-Venezia S. 2010. Complete nucleotide sequence of KPC-3-encoding plasmid pKpQIL in the epidemic *Klebsiella pneumoniae* sequence type 258. *Antimicrob Agents Chemother* 54:4493–4496. <https://doi.org/10.1128/AAC.00175-10>.
  10. Bowers JR, Kitchel B, Driebe EM, MacCannell DR, Roe C, Lemmer D, de Man T, Rasheed JK, Engelthaler DM, Keim P, Limbago BM. 2015. Genomic analysis of the emergence and rapid global dissemination of the clonal group 258 *Klebsiella pneumoniae* pandemic. *PLoS One* 10:e0133727. <https://doi.org/10.1371/journal.pone.0133727>.
  11. Shields RK, Clancy CJ, Hao B, Chen L, Press EG, Iovine NM, Kreiswirth BN, Nguyen MH. 2015. Effects of *Klebsiella pneumoniae* carbapenemase subtypes, extended-spectrum beta-lactamases, and porin mutations on the in vitro activity of ceftazidime-avibactam against carbapenem-resistant *K. pneumoniae*. *Antimicrob Agents Chemother* 59:5793–5797. <https://doi.org/10.1128/AAC.00548-15>.
  12. De Majumdar S, Yu J, Fookes M, McAteer SP, Llobet E, Finn S, Spence S, Monahan A, Kissenpennig A, Ingram RJ, Bengoechea J, Gally DL, Fanning S, Elborn JS, Schneiders T. 2015. Elucidation of the RamA regulon in *Klebsiella pneumoniae* reveals a role in LPS regulation. *PLoS Pathog* 11:e1004627. <https://doi.org/10.1371/journal.ppat.1004627>.
  13. Castanheira M, Mills JC, Costello SE, Jones RN, Sader HS. 2015. Ceftazidime-avibactam activity tested against *Enterobacteriaceae* isolates from U.S. hospitals (2011 to 2013) and characterization of beta-lactamase-producing strains. *Antimicrob Agents Chemother* 59:3509–3517. <https://doi.org/10.1128/AAC.00163-15>.
  14. Castanheira M, Mendes RE, Sader HS. 2016. Low frequency of ceftazidime-avibactam resistance among *Enterobacteriaceae* isolates carrying *bla<sub>KPC</sub>* collected in hospitals from the United States from 2012 to 2015. *Antimicrob Agents Chemother* 61:e02369-16. <https://doi.org/10.1128/AAC.02369-16>.
  15. Aitken SL, Tarrand JJ, Deshpande LM, Tverdek FP, Jones AL, Shelburne SA, Prince RA, Bhatti MM, Rolston KV, Jones RN, Castanheira M, Chemaly RF. 2016. High rates of nonsusceptibility to ceftazidime-avibactam and identification of New Delhi metallo-beta-lactamase production in *Enterobacteriaceae* bloodstream infections at a major cancer center. *Clin Infect Dis* 63:954–958. <https://doi.org/10.1093/cid/ciw398>.
  16. Shields RK, Chen L, Cheng S, Chavda KD, Press EG, Snyder A, Pandey R, Doi Y, Kreiswirth BN, Nguyen MH, Clancy CJ. 2016. Emergence of ceftazidime-avibactam resistance due to plasmid-borne *blaKPC-3* mutations during treatment of carbapenem-resistant *Klebsiella pneumoniae* infections. *Antimicrob Agents Chemother* <https://doi.org/10.1128/AAC.02097-16>.
  17. Shields RK, Potoski BA, Haidar G, Hao B, Doi Y, Chen L, Press EG, Kreiswirth BN, Clancy CJ, Nguyen MH. 2016. Clinical outcomes, drug toxicity, and emergence of ceftazidime-avibactam resistance among patients treated for carbapenem-resistant *Enterobacteriaceae* Infections. *Clin Infect Dis* 63:1615–1618. <https://doi.org/10.1093/cid/ciw636>.
  18. Martinez-Martinez L. 2008. Extended-spectrum beta-lactamases and the permeability barrier. *Clin Microbiol Infect* 14(Suppl 1):S82–S89. <https://doi.org/10.1111/j.1469-0691.2007.01860.x>.
  19. Grobner S, Linke D, Schutz W, Fladerer C, Madlung J, Autenrieth IB, Witte W, Pfeifer Y. 2009. Emergence of carbapenem-nonsusceptible extended-spectrum beta-lactamase-producing *Klebsiella pneumoniae* isolates at the university hospital of Tubingen, Germany. *J Med Microbiol* 58:912–922. <https://doi.org/10.1099/jmm.0.005850-0>.
  20. Findlay J, Hamouda A, Dancer SJ, Amyes SG. 2012. Rapid acquisition of decreased carbapenem susceptibility in a strain of *Klebsiella pneumoniae* arising during meropenem therapy. *Clin Microbiol Infect* 18:140–146. <https://doi.org/10.1111/j.1469-0691.2011.03515.x>.
  21. Shen Z, Ding B, Ye M, Wang P, Bi Y, Wu S, Xu X, Guo Q, Wang M. 2017. High ceftazidime hydrolysis activity and porin OmpK35 deficiency contribute to the decreased susceptibility to ceftazidime/avibactam in KPC-producing *Klebsiella pneumoniae*. *J Antimicrob Chemother* <https://doi.org/10.1093/jac/dkx066>.
  22. CLSI. 2017. Performance standards for antimicrobial susceptibility testing M100S, 27th ed. Clinical and Laboratory Standards Institute, Wayne, PA.
  23. Zankari E, Hasman H, Cosentino S, Vestergaard M, Rasmussen S, Lund O, Aarestrup FM, Larsen MV. 2012. Identification of acquired antimicrobial resistance genes. *J Antimicrob Chemother* 67:2640–2644. <https://doi.org/10.1093/jac/dks261>.
  24. Carattoli A, Zankari E, Garcia-Fernandez A, Voldby Larsen M, Lund O, Villa L, Moller Aarestrup F, Hasman H. 2014. In silico detection and typing of plasmids using PlasmidFinder and plasmid multilocus sequence typing. *Antimicrob Agents Chemother* 58:3895–3903. <https://doi.org/10.1128/AAC.02412-14>.
  25. Afgan E, Baker D, van den Beek M, Blankenberg D, Bouvier D, Cech M, Chilton J, Clements D, Coraor N, Eberhard C, Gruning B, Guerler A, Hillman-Jackson J, Von Kuster G, Rasche E, Soranzo N, Turaga N, Taylor J, Nekrutenko A, Goecks J. 2016. The Galaxy platform for accessible, reproducible and collaborative biomedical analyses: 2016 update. *Nucleic Acids Res* 44:W3–W10. <https://doi.org/10.1093/nar/gkw343>.
  26. Blankenberg D, Gordon A, Von Kuster G, Coraor N, Taylor J, Nekrutenko A, Galaxy T. 2010. Manipulation of FASTQ data with Galaxy. *Bioinformatics* 26:1783–1785. <https://doi.org/10.1093/bioinformatics/btq281>.
  27. Yuan JS, Reed A, Chen F, Stewart CN, Jr. 2006. Statistical analysis of real-time PCR data. *BMC Bioinformatics* 7:85. <https://doi.org/10.1186/1471-2105-7-85>.
  28. Bustin SA, Benes V, Garson JA, Hellemans J, Huggett J, Kubista M, Mueller R, Nolan T, Pfaffl MW, Shipley GL, Vandesompele J, Wittwer CT. 2009. The MIQE guidelines: minimum information for publication of quantitative real-time PCR experiments. *Clin Chem* 55:611–622. <https://doi.org/10.1373/clinchem.2008.112797>.